

Cite this: *Chem. Commun.*, 2019, 55, 2277Received 19th November 2018,  
Accepted 29th January 2019

DOI: 10.1039/c8cc09188a

rsc.li/chemcomm

# Tuning the reduction potential of quinones by controlling the effects of hydrogen bonding, protonation and proton-coupled electron transfer reactions†

Raymond R. S. Shi,<sup>a</sup> Malcolm E. Tessensohn,<sup>b</sup> Sherman J. L. Lauw,<sup>a</sup>  
Nicolette A. B. Y. Foo<sup>a</sup> and Richard D. Webster<sup>id</sup> \*<sup>a,b</sup>

An all-organic cell comprising 2,3-dimethyl-1,4-naphthoquinone and pyrano[3,2-*f*]chromene as electroactive elements exhibited a good combination of large cell voltage and stability of the reduced quinone upon the addition of diethyl malonate (a weak organic acid), as compared to the addition of trifluoroethanol (which led to a high cell potential but low stability *via* strong hydrogen bonding interactions) and the addition of trifluoroacetic acid (which led to a lower cell potential but high stability through proton transfer).

The utility of electricity as a low carbon form of energy when obtained through renewable energy sources has fuelled tremendous interest in the development of efficient electrical energy storage devices, where work is aimed at improving cell voltage and stability, energy density and round-trip efficiency, and suppressing capacity fading, among other factors.<sup>1–8</sup> Organic compounds are useful in providing a large range of cell voltages because their chemical and redox properties can be easily modified *via* functionalization. A fully organic redox flow battery (RFB) can thus be prepared together with an organic solvent, organic supporting electrolyte and non-metallic electrodes. The major drawbacks of molecularly based RFBs, however, are the generation of radicals and other highly reactive charged species that may compromise the stability and, consequently, lifetime of the battery.

Quinone and pyranochromene compounds are useful for this purpose. Firstly, both exhibit simple electrochemical behaviour in organic solvents. In an aprotic organic solvent like CH<sub>3</sub>CN, 2,3-dimethyl-1,4-naphthoquinone (VKA), an analogue of vitamin K<sub>1</sub>, typically undergoes two one-electron reduction reactions (*i.e.* EE mechanism where E represents an electron-transfer step) to first give the radical anion (VKA<sup>•−</sup>) at −1.22 V vs. Fc/Fc<sup>+</sup> ( $E^{\text{red}(1)}$ ) and subsequently the aromatic dianion (VKA<sup>2−</sup>) at −1.76 V vs. Fc/Fc<sup>+</sup> ( $E^{\text{red}(2)}$ )

<sup>a</sup> Division of Chemistry & Biological Chemistry, School of Physical and Mathematical Sciences, Nanyang Technological University, 21 Nanyang Link, 637371, Singapore. E-mail: Webster@ntu.edu.sg

<sup>b</sup> Environmental Chemistry and Materials Centre, Nanyang Environment & Water Research Institute, 1 Cleantech Loop, CleanTech One #06-10, 637141, Singapore

† Electronic supplementary information (ESI) available: Experimental procedures and discussion. See DOI: 10.1039/c8cc09188a

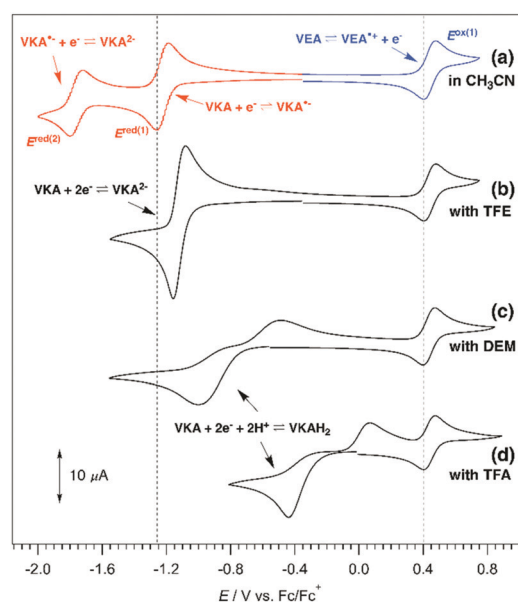
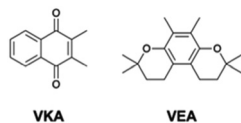


Fig. 1 Cyclic voltammograms of 2 mM VKA and VEA with 0.2 M *n*Bu<sub>4</sub>NPF<sub>6</sub> as the supporting electrolyte in CH<sub>3</sub>CN (a) only, and with (b) 200 mM TFE, (c) 400 mM DEM and (d) 100 mM TFA. The voltammograms were recorded on a 1 mm diameter planar disk glassy carbon working electrode at a scan rate of 0.1 V s<sup>−1</sup> at 25 ± 2 °C.

(Fig. 1a, red trace).<sup>9–15</sup> An analogue of vitamin E, pyrano[3,2-*f*]chromene (VEA), on the other hand, only undergoes a one-electron oxidation reaction to its radical cation (VEA<sup>•+</sup>) at +0.45 V vs. Fc/Fc<sup>+</sup> ( $E^{\text{ox}(1)}$ ) (Fig. 1a, blue trace).<sup>16</sup> The structures of both compounds are shown in Scheme 1.

Secondly, the electron-transfer processes of both compounds show good chemical reversibility on the timescale of cyclic voltammetry experiments (seconds) and so enables them to potentially serve as electroactive compounds in batteries, to which the theoretical maximum cell voltage obtainable is 2.21 V (from  $E_{\text{cell}} = E_{\text{cathode}} - E_{\text{anode}} = E^{\text{ox}(1)} - E^{\text{red}(2)}$ ). The stability of the cell in pure CH<sub>3</sub>CN, which is typically measured on the scale of days and months for RFBs, is however quite poor owing to the high



**Scheme 1** 2,3-Dimethyl-1,4-naphthoquinone (left) and pyrano[3,2-*f*]chromene (right).

reactivity of the dianion  $VKA^{2-}$  (likely due to reactions with trace oxygen or water). Cell stability under electrolysis timescales (>minutes) can nevertheless be improved through stabilization of  $VKA^{•-}$  and  $VKA^{2-}$  by purely hydrogen bonding with trifluoroethanol (TFE) (Fig. 1b) or purely protonation from trifluoroacetic acid (TFA) (Fig. 1d), or possibly a combination of both (hydrogen bonding and proton transfer) with diethyl malonate (DEM) (Fig. 1c), which facilitates the reduction of VKA and shifts the reduction potentials to less negative values. The oxidation of VEA appears to be unaffected by the addition of TFE, DEM and TFA (*i.e.* no change in  $E^{ox(1)}$ ) so indicating that VEA and  $VEA^{•+}$  are less affected by hydrogen-bonding and proton-transfer reactions.

Hydrogen bonding between VKA and TFE results in the gradual shifting of the reduction processes  $E^{red(1)}$  and  $E^{red(2)}$  towards more positive values; this occurs over a wide concentration range and is dependent on the extent of the interaction (see Fig. 2a).<sup>17–21</sup> The shifts in  $E^{red(2)}$  are greater than those of  $E^{red(1)}$  which result in the formation of a single two-electron reduction process when sufficient amounts of TFE are present (*ca.* 50 equivalents), through the merger of the individual one-electron reduction reactions, that converts VKA directly into  $VKA^{2-}$ . Despite the noticeable changes in the cyclic voltammograms, the EE reduction mechanism remains unaffected by hydrogen bonding. These shifts in reduction potential of quinones in organic solvents have been studied extensively during the addition of water, which also undergoes relatively strong hydrogen-bonding interactions with the semiquinones and especially dianions.<sup>18–20</sup> The series of possible consecutive electron-transfer and hydrogen-bonding reactions associated with the chemically reversible transformation between VKA and its hydrogen-bonded dianion,  $[VKA(TFE)_2]^{2-}$ , can be more accurately described by the electrochemical “square-scheme” mechanism shown in Scheme 2, where the electron-transfer reactions are drawn horizontally and the hydrogen-bonding reactions are given vertically. Scheme 2 can be extended vertically to include more hydrogen-bonding interactions.

Protonation can be viewed as an extreme case of hydrogen bonding where the interaction between the hydrogen donor and hydrogen acceptor is so strong that the hydrogen nuclei is completely transferred. The addition of small amounts of TFA to the VKA containing solution resulted in an immediate large shift in the  $E^{red(1)}$  and  $E^{red(2)}$  processes (Fig. 2b), which is due to strong hydrogen bonding with VKA and protonation of the reduced forms. The dihydroquinone  $VKAH_2$  is obtained as the final product, to which the overall two-electron two-proton reduction may proceed either through the EC<sub>2</sub>C or EC<sub>2</sub>CE pathway. The other distinctions of protonation compared to hydrogen bonding (where there is no transfer of protons to the

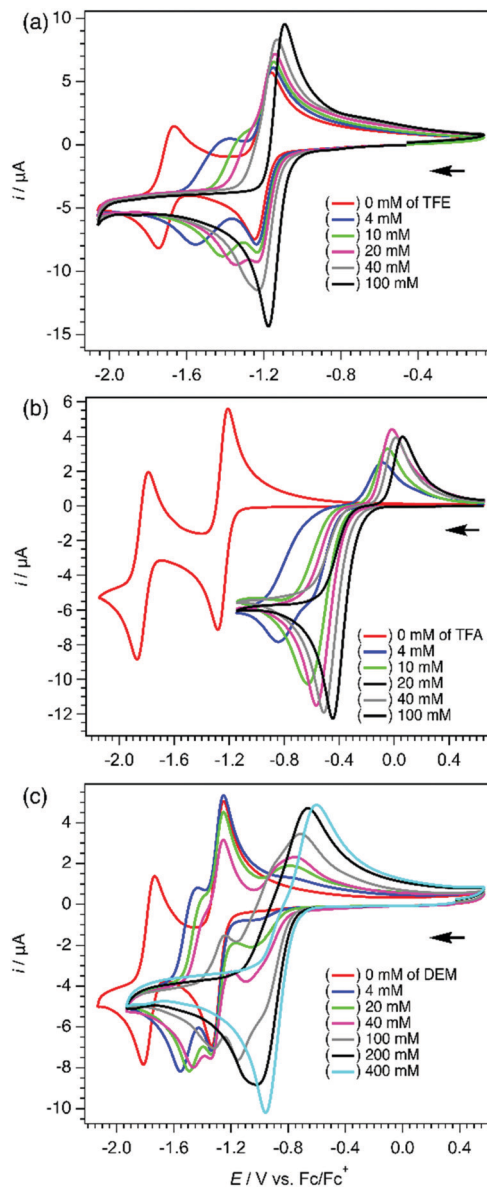
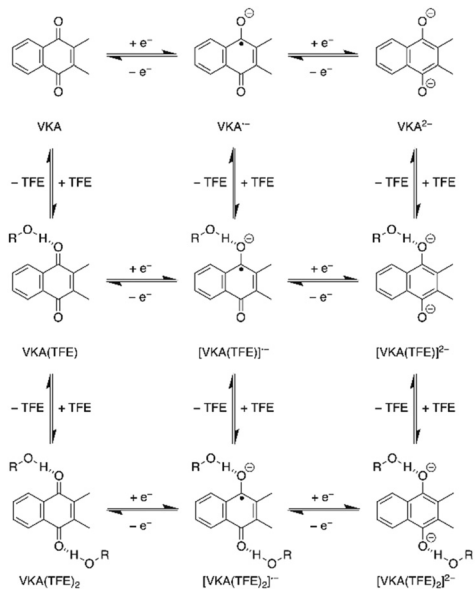
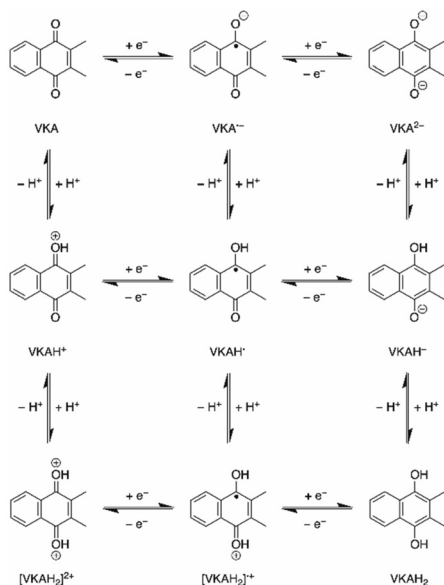


**Fig. 2** Cyclic voltammograms of 2 mM VKA/0.2 M  $nBu_4NPF_6$  in  $CH_3CN$  recorded with a 1 mm diameter planar disk glassy carbon working electrode at  $0.1 V s^{-1}$  at  $25 \pm 2^\circ C$  at different concentrations of (a) TFE, (b) TFA and (c) DEM.

reduced quinone) are the occurrence of the reduction of VKA at potentials that are significantly more positive (*cf.* Fig. 1b and d), with lower concentrations of the acid, a marked increase in the  $E^{red}$  to  $E^{ox}$  separation as well as slowed heterogeneous electron-transfer rates (see Fig. 2b).<sup>22,23</sup> The electrochemical “square-scheme” in Scheme 3, which is analogous to Scheme 2, shows the sequence of electron-transfer (drawn horizontally) and proton-transfer (given vertically) reactions that VKA can undergo during its chemically reversible transformation into  $VKAH_2$  in the presence of high amounts of acid. No change in the UV-vis spectra of the starting material was observed in the absence and presence of up to 5 M TFA, suggesting that the VKA does not undergo immediate protonation with acid (Fig. S1 in the ESI†).



**Scheme 2** Electrochemical "square-scheme" mechanism for the reduction of VKA with hydrogen bonding to TFE. R =  $\text{CH}_2\text{CF}_3$ .



**Scheme 3** Electrochemical "square-scheme" mechanism for the reduction of VKA with proton-transfer reactions.

The cyclic voltammograms in Fig. 1 and approximate  $E_{\text{cell}}$  values of 1.56, 1.18 and 0.61 V obtained in the presence of TFE, DEM and TFA, respectively, (where  $E_{\text{cell}} = E^{\text{ox}(1)} - E^{\text{red}(1)}$ ) indicate that hydrogen bonding between VKA and TFE gives the largest cell potential by *ca.* 950 mV more than that obtained through protonation by TFA. The hydrogen-bonded dianion  $[\text{VKA}(\text{TFE})_2]^{2-}$  was however found to be less stable than  $\text{VKAH}_2$ , and so undermines the applicability of TFE for use in an all-organic battery. The stabilities of VKA and its reduced products,  $[\text{VKA}(\text{TFE})_2]^{2-}$  and  $\text{VKAH}_2$ , were determined through a comparison of the peak reduction currents from the cyclic voltammograms as well as

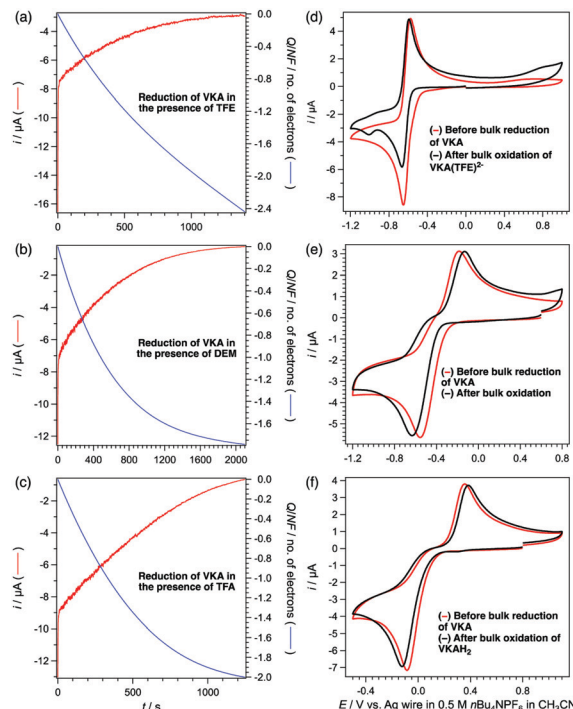
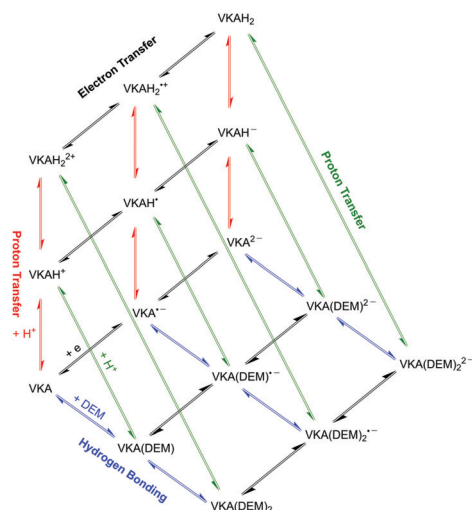


**Fig. 3** (a–c) Coulometric data for the reductive controlled potential electrolysis of 2 mM VKA/0.2 M  $n\text{Bu}_4\text{NPF}_6$  in  $\text{CH}_3\text{CN}$  in the presence of (a) 200 mM TFE, (b) 100 mM TFA and (c) and 400 mM DEM. The  $i$  vs.  $t$  and no. of electrons transferred vs.  $t$  plots are shown in red and blue, respectively. (d–f) Corresponding cyclic voltammograms recorded with a 1 mm diameter planar disk glassy carbon working electrode at  $0.1 \text{ V s}^{-1}$  at  $25 \pm 2 \text{ }^\circ\text{C}$  before the bulk reduction of VKA (red) and after the bulk oxidation of reduced VKA (*i.e.* hydrogen-bonded  $\text{VKA}^{2-}$  or  $\text{VKAH}_2$ ) (black) in the presence of (d) 200 mM TFE, (e) 100 mM TFA and (f) and 400 mM DEM.

UV-vis spectra (see Fig. S2 in the ESI† for TFA and DEM) recorded at the start and upon completion of the controlled potential electrolysis experiments. The voltammetric peak currents for  $[\text{VKA}(\text{TFE})_2]^{2-}$  recorded immediately after the electrolysis were noticeably smaller than prior to electrolysis as shown in Fig. 3d. However, for  $\text{VKAH}_2$ , the voltammetric peak currents showed a negligible change over the course of the electrolysis experiments (Fig. 3e). The applied potential needed for exhaustive reduction of VKA decreased in the presence of the additives in the order  $\text{TFA} < \text{DEM} < \text{TFE}$ , and this potential decrease can be correlated to improving the stability of the reduced quinone *via* the lowered reactivity of the product (the exact applied potentials and experimental details of the electrolysis are given in the ESI,†).

For the experiments with DEM, the electrochemical reduction of VKA appears to show features of hydrogen bonding at low ( $< 10 \text{ mM}$ ) concentrations of DEM (*i.e.* two one-electron reduction behaviour with  $E^{\text{red}(2)}$  shifted, yet no change in the chemical reversibility of both processes) as well as protonation at high ( $> 20 \text{ mM}$ ) concentrations of DEM (*i.e.* a single reduction process accompanied by a broad reverse oxidation peak) (Fig. 2c). Since DEM is a weak acid and does not fully dissociate in  $\text{CH}_3\text{CN}$ , it is likely that the reduction of VKA in the presence of DEM involves a combination of proton-coupled



**Scheme 4** Electrochemical “wedge-scheme” mechanism for the reduction of VKA with hydrogen bonding and proton-transfer reactions with DEM.

electron transfer (PCET)<sup>24–30</sup> and hydrogen bonding through a “wedge-scheme” type (Scheme 4)<sup>31</sup> mechanism. In the PCET pathway, the proton and electron may be transferred concertedly (that would be represented in Scheme 3 by a series of diagonal arrows) or in a stepwise fashion.

The “wedge-scheme” mechanism in Scheme 4 may be viewed as an intermediate scenario lying between Schemes 2 and 3 where both hydrogen bonding (blue reaction arrows) and protonation (red reaction arrows) simultaneously occur, with hydrogen bonding favoured at lower concentrations of DEM and with the neutral VKA, while protonation supersedes at higher concentrations of DEM and preferentially involves the dianion  $VKA^{2-}$ . A direct transformation between the protonated and hydrogen-bonded states may also occur *via* equilibrium proton-transfer reactions (represented by the green reaction arrows). The exact pathway undertaken in the “wedge-scheme” mechanism is highly dependent on the combination of the basicity of the quinone, acidity of the hydrogen donor, their concentrations as well as type of solvent used. Most importantly, the addition of easily controlled amounts of DEM allowed the potential of the two-electron reduction of the quinone to be optimised, so that a larger  $E_{\text{cell}}$  value (*i.e.* about two times that obtained with TFA) and excellent compound stability were achieved (voltammograms and UV-vis spectra recorded before bulk electrolysis and after complete discharge did not show any unexpected changes over a 24 hour period; see Fig. S3 in the ESI†).

The results of this study show that the nature and amount of the additive is critical in determining the reduction mechanism as well as for achieving a combination of good stability and large cell potential for organic solvent based RFBs that utilize quinones as the anolyte. Work is presently ongoing in our laboratory to develop an all-organic RFB for commercial use.

This work was supported by a Singapore Government MOE Academic Research Fund Tier 1 Grant (RG109/15). R. R. S. S. thanks Nanyang Technological University for the award of a NTU Research Scholarship.

## Conflicts of interest

There are no conflicts to declare.

## Notes and references

- 1 L. Li, S. Kim, W. Wang, M. Vijayakumar, Z. Nie, B. Chen, J. Zhang, G. Xia, J. Hu, G. Graff, J. Liu and Z. Yang, *Adv. Energy Mater.*, 2011, **1**, 394.
- 2 P. Alotto, M. Guarnieri and F. Moro, *Renewable Sustainable Energy Rev.*, 2014, **29**, 325.
- 3 S. P. S. Badwal, S. S. Giddey, C. Munnings, A. I. Bhatt and A. F. Hollenkamp, *Front. Chem.*, 2014, **2**, 79.
- 4 B. Yang, L. Hooper-Burkhardt, F. Wang, G. K. S. Prakash and S. R. Narayanan, *J. Electrochem. Soc.*, 2014, **161**, A1371.
- 5 K. Gong, Q. Fang, S. Gu, S. Y. L. Fong and Y. Yan, *Energy Environ. Sci.*, 2015, **8**, 3515.
- 6 X. Luo, J. Wang, M. Dooner and J. Clarke, *Appl. Energy*, 2015, **137**, 511.
- 7 K. Wedege, E. Dražević, D. Konya and A. Bentien, *Sci. Rep.*, 2016, **6**, 39101.
- 8 J. Winsberg, T. Hagemann, T. Janoschka, M. D. Hager and U. S. Schubert, *Angew. Chem., Int. Ed.*, 2017, **56**, 686.
- 9 B. Uno, A. Kawabata and K. Kano, *Chem. Lett.*, 1992, 1017.
- 10 N. Gupta and H. Linschitz, *J. Am. Chem. Soc.*, 1997, **119**, 6384.
- 11 M. Aguilar-Martínez, N. A. Macías-Ruvalcaba and I. González, *J. Mex. Chem. Soc.*, 2000, **44**, 74.
- 12 M. Gómez, F. J. González and I. González, *Electroanalysis*, 2003, **15**, 635.
- 13 M. Aguilar-Martínez, N. A. Macías-Ruvalcaba, J. A. Bautista-Martínez, M. Gómez, F. J. González and I. González, *Curr. Org. Chem.*, 2004, **8**, 1721.
- 14 B. Jin, J. Huang, A. Zhao, S. Zhang, Y. Tian and J. Yang, *J. Electroanal. Chem.*, 2010, **650**, 116.
- 15 J. Katsumi, T. Nakayama, Y. Esaka and B. Uno, *Anal. Sci.*, 2012, **28**, 257.
- 16 H. M. Peng, B. F. Choules, W. W. Yao, Z. Zhang, R. D. Webster and P. M. W. Gill, *J. Phys. Chem. B*, 2008, **112**, 10367.
- 17 S. Hayano and M. Fujihira, *Bull. Chem. Soc. Jpn.*, 1971, **44**, 2051.
- 18 Y. Hui, E. L. K. Chng, C. Y. L. Chng, H. L. Poh and R. D. Webster, *J. Am. Chem. Soc.*, 2009, **131**, 1523.
- 19 Y. Hui, E. L. K. Chng, L. P.-L. Chua, W. Z. Liu and R. D. Webster, *Anal. Chem.*, 2010, **82**, 1928.
- 20 M. E. Tessensohn, H. Hirao and R. D. Webster, *J. Phys. Chem. C*, 2013, **117**, 1081.
- 21 M. E. Tessensohn, M. Lee, H. Hirao and R. D. Webster, *ChemPhysChem*, 2015, **16**, 160.
- 22 H.-S. Kim, T. D. Chung and H. Kim, *J. Electroanal. Chem.*, 2001, **498**, 209.
- 23 J. Kim, T. D. Chung and H. Kim, *J. Electroanal. Chem.*, 2001, **499**, 78.
- 24 C. Costentin, M. Robert and J.-M. Savéant, *J. Am. Chem. Soc.*, 2006, **128**, 8726.
- 25 C. Costentin, M. Robert and J.-M. Savéant, *J. Am. Chem. Soc.*, 2006, **128**, 4552.
- 26 C. Costentin, *Chem. Rev.*, 2008, **108**, 2145.
- 27 C. Costentin, M. Robert and J.-M. Savéant, *Acc. Chem. Res.*, 2010, **43**, 1019.
- 28 C. Costentin, M. Robert and J.-M. Savéant, *Phys. Chem. Chem. Phys.*, 2010, **12**, 11179.
- 29 C. Costentin, M. Robert, J.-M. Savéant and C. Tard, *Angew. Chem., Int. Ed.*, 2010, **49**, 3803.
- 30 J.-M. Savéant and C. Tard, *J. Am. Chem. Soc.*, 2014, **136**, 8907.
- 31 B. T. Tamashiro, M. R. Cedano, A. T. Pham and D. K. Smith, *J. Phys. Chem. C*, 2015, **119**, 12865.